Phase analysis of Australian uranium ore concentrates determined by variable temperature synchrotron powder X-Ray diffraction

Samantha B. Pandelus[1], Brendan J. Kennedy[2,*], Gabriel Murphy[2,3+], Helen E. Brand[4], Elizabeth Keegan[3], Allan Pring[1,5], Rachel S. Popelka-Filcoff[1,6]

1. College of Science and Engineering, Flinders University, Adelaide SA 5001, Australia
2. School of Chemistry, The University of Sydney, Sydney, NSW 2006, Australia
3. ANSTO, Lucas Heights, NSW 2234, Australia
4. Australian Synchrotron, 800 Blackburn Road, Clayton, Victoria 3168, Australia
5. School of Physical Sciences, University of Adelaide, Adelaide SA 5005, Australia
6. School of Geography, Earth and Atmospheric Sciences, University of Melbourne, VIC 3010 Australia

+ Present address: *Institute of Energy and Climate Research (IEK-6), Forschungszentrum Jülich GmbH, 52428 Jülich, Germany*

Address correspondence to Brendan Kennedy (Brendan.Kennedy@Sydney.edu.au)

Abstract

The chemical speciation of uranium oxides is sensitive to the provenance of the samples and their storage conditions. Here we use diffraction methods to characterise the phases found in three aged (> 10 years) uranium ore concentrates of different origins as well as *in situ* analysis of the thermally induced structural transitions of these materials. The structures of the crystalline phases found in the three samples have been refined, using high resolution synchrotron X-ray diffraction data. Rietveld analysis of the samples from the Olympic Dam and Ranger uranium mines has revealed the presence of crystalline α-$UO_2(OH)_2$, together with metaschoepite $(UO_2)_4O(OH)_6{\cdot}5H_2O$, in the aged U_3O_8 samples, and it is speculated that this forms as a consequence of the corrosion of the U_3O_8 in the presence of metaschoepite. The third sample, from the Beverley uranium mine was peroxide, $[UO_2(\eta^2\text{-}O_2)(H_2O)_2]$ (metastudtite) altered α-$UO_2(OH)_2$ and metaschoepite. A core-shell model is proposed

to account for the broadening of the diffraction peaks of the U_3O_8 evident in the samples.

Introduction

The formation and transformation of uranium oxides are of considerable technological and scientific interest reflecting the role of uranium in the nuclear fuel cycle. There is the additional complication of radioactive materials being diverted for nefarious purposes.[1, 2] Uranium ore concentrate (UOC) is the feedstock for the nuclear fuel cycle and its production is dominated by a relatively small number of countries, notably Canada, Namibia, Australia, and Kazakhstan. Conventionally, the term yellow cake has been used to describe UOC regardless of its origin and color, yet each facility produces UOC with unique characteristics, including phase composition, chemical and isotopic distributions that can be used to identify its provenance.[1, 3-5] To investigate illicitly trafficked nuclear material or nuclear material found outside of regulatory control, it is crucial to identify the origin of the material and a range of characterization methods including chemical and structural analysis have been employed. In a recent X-ray diffraction study of 15 UOC samples, Su *et al.* found 11 different crystalline phases, with the majority of samples studied containing two or more crystalline phases.[6] It has been documented that chemical speciation of uranium oxides can change with age, and is sensitive to the temperature and relative humidity during storage.[7, 8] Structural analysis may be valuable for characterising material provenance and may provide insight into its storage over time.

Australia is the world's third largest producer of uranium and it exports approximately 7000 tons of UOC per annum from three active, or recently active, uranium mines namely the Olympic Dam, Ranger and Beverley mines. The ore at each mine varies in mineralogy, minor and trace element geochemistry and these are further impacted by differences in mining procedures as well as ore processing methods and on the customer needs and regulation requirements. The final step in the production of the UOC at both the Olympic Dam and Ranger mines is roasting (calcining) and this results in the formation of U_3O_8. At the Beverley mine the product is $UO_4.2H_2O$ precipitated by the addition of peroxide. Keegan *et al.*[9] determined the concentrations of 40 minor and trace elements in UOC from these three Australian mines and was able

to use this information to build characteristic elemental and isotope signatures for the samples. Ditcham and co-workers,[10] working with the same bulk samples as Keegan [9] demonstrated that a combination of differential thermal analysis (DTA), thermogravimetric analysis (TGA) and powder X-ray diffraction (PXRD) could be used to differentiate between the original sources, however a number of the minor phases in the UOCs could not be fully characterized. An interesting observation in that work was that the temperature at which various intermediate phases formed during the thermal decomposition measurements depended on the origin of the sample. Other studies on the thermal decomposition of a number of UOC phases have been reported and although it is generally agreed that the final product of calcination is either U_3O_8 or UO_2 depending on the atmosphere, there is little consensus regarding the nature of any intermediate phases.[11]

The anthropogenic corrosion of uranium oxide compounds is well known and can lead to a complex mixture of hydrate uranium oxides.[12, 13] For example Sweet *et al.*,[14] reported that UO_3 is unstable when exposed to moisture and will transform to $UO_2(OH)_2$, and that when this is heated to above 450 °C it dehydrates to γ-UO_3.[15] Many of the hydrated uranium materials formed are related to the schoepite group with the general formula of $UO_3 \cdot 2H_2O$. Wilkerson *et al.* recently showed that crystalline α-UO_3 material converted to schoepite upon storage.[16] Similarly Hanson *et al*. observed the conversion of amorphous UO_3 to schoepite on storage, a process that was sensitive to ageing time, temperature and relative humidity.[17] The surface morphology of uranium oxides is impacted on storage and methods to like surface morphology to the processing history and storage of uranium oxides have been reported.[18, 19] The oxidation and hydration of U_3O_8 can lead to the formation of schoepite phases thus with time and exposure to moisture the phase assemblage of a UOC will evolve.[8, 20] Schoepite is assumed to easily transition to meta-schoepite under ambient conditions and it has also been shown that metaschoepite can form on the surface of U_3O_8 when exposed to air and moisture.[21]

The accurate identification of secondary uranium oxide phases can be very challenging using laboratory-based diffractometers.[6] In the current study the major phases present within three UOC samples and the temperature induced phase transitions of these were determined using high energy monochromatic X-ray measurements from synchrotron radiation. The energy was selected to minimize absorption from the

sample and particularly to avoid the effects of the U L-absorption edges. The extended *d*-range accessible using high energies allows precise and accurate structural data to be refined. In this study we explore the change in the phase composition in UOCs brought about by the absorption of moisture during prolonged storage (12 to 14 years). From this data we can accurately calculate the amount of structurally bound water and follow of the evolution of the phases of the Australian UOC characterised by Keegan *et al.*[9]

Experimental

Samples

The samples used in this study were from the same bulk sample lots studied by Keegan *et al*. and were made available by the Australian Nuclear Science and Technology Organization (ANSTO).[9] The Ranger mine sample, NFS13-091, was received by ANSTO in October 2004, and collected by the mine operators in the period 2003/2004. The Beverley mine sample, NFS13-088, was received by ANSTO in September 2004 and collected by the mine operators in 2003/2004. The Olympic Dam mine sample, NSF13-094, was received by ANSTO in February 2006 and was collected by the mine operators in 2005. The UOC produced at the Ranger and Olympic Dam mines is described as U_3O_8 and at the time of initial receipt by ANSTO and the current analysis, in 2017, both samples appeared dark green to black in colour. The Beverley mine UOC is nominally $UO_4.2H_2O$ and was yellow/orange in colour on receipt at ANSTO and in 2017. Further details and the production methods for the UOC samples are given elsewhere. [9, 10] The samples were stored in the containers in which they were collected at the respective mine sites, either plastic screw-top bottles or zip-lock bags. Each container was placed within secondary containment (another zip-lock bag) and stored in a cupboard in an air-conditioned laboratory (22 °C, relative humidity 40 %) and only opened for sub-sampling on several occasions over the ~10 year period. All of the samples for the synchrotron experiments were loaded into capillaries in mid-September 2017 and data were collected shortly thereafter.

Instrumental and Data analysis

Preliminary X-ray diffraction patterns were collected for the three samples in 2006, shortly after they were supplied by the mining companies. Patterns were collected on a Philips PW1050 X-ray diffractometer (PANalytical Ltd., Almelo, Netherlands) with Cu Kα radiation; data were collected over the angular range $5° \leq 2\theta \leq 100°$ with a

step size of 0.05° and acquisition times of 5 s per step. The data measured in 2015 used a Bruker D8 X-ray diffractometer (Billerica, Massachusetts, USA) with a Cu X-ray tube (1.5418 Å) (40 kV, 40 mA) and a diffraction angle range of $10° \leq 2\theta \leq 150°$with a step size of 0.02° and a counting time of 20 s per step. Samples were adhered onto double-sided carbon tape and mounted on Si single crystals in preparation for XRD analysis.

Finely ground sub-samples of the UOC samples were placed in 0.2 mm quartz glass capillaries that were then flame sealed. Synchrotron X-ray diffraction (S-XRD) data were measured on the powder diffraction (PD) beamline at the Australian Synchrotron operating at around 16 keV (0.728938 Å based on calibrations using a NIST LaB_6 (660b) standard reference) using an array of 16 MYTHEN II microstrip detectors.[22] Each sample was heated from 25 to 875 °C with a ramp rate of 5 °C per minute and patterns were collected at 25 °C intervals. Data collection was commenced after a 60 second thermal equilibration period. Temperature was controlled using an FMB-Oxford hot air blower placed below the capillary. A smaller number of datasets were collected on the cooling cycle where a cooling rate of 10 °C per minute was employed. The structures were refined against the S-XRD data by the Rietveld method as implemented in the program GSAS with the EXPGUI frontend.[23, 24] The peak shapes were modelled using a pseudo-Voigt function and the background was estimated using a shifted Chebyschev function. The scale factor, detector zero-point, lattice parameters, atomic coordinates and isotropic atomic displacement parameters were refined together with the peak profile parameters.

Results and Discussion

Preliminary X-ray analysis

Analysis of the preliminary X-ray data, recorded in 2006, using the Rietveld method, revealed that the crystalline material in the samples from the Ranger and Olympic Dam mines was orthorhombic U_3O_8 and within the sensitivity of the data both samples were single phase. There was no evidence in the data for the presence of any hydrated species. The diffraction pattern of the sample from the Beverley mine was distinctly different and could be fitted to a $UO_4 \cdot 2H_2O$ model. Rietveld analysis revealed a number of weak unfitted reflections that could be indexed to the presence of

metaschoepite $(UO_2)_4O(OH)_6{\cdot}5H_2O$; sometimes described as $UO_3{\cdot}2H_2O$. The starting models used in the Rietveld refinements were taken from the literature: for metaschoepite we used Weller *et al.* [25], for orthorhombic U_3O_8 Loopstra [26] and for metastudtite we utilised the orthorhombic model developed by Weck *et al.*[27] The phase composition was estimated to be $UO_4{\cdot}2H_2O$, 95.9(5)wt % and α-$(UO_2)_4O(OH)_6{\cdot}5H_2O$ 4.1(3) wt % with $\chi 2 = 2.34$. Refinements against the Beverley data with a single-phase model gave $\chi\ 2 = 2.58$. As will be demonstrated below, during storage these UOC samples underwent partial alteration due to interaction with atmospheric moisture.

Room Temperature Structure and Phases

Figure 1 shows Rietveld refinements for diffraction profiles measured at 25 °C for each of the three UOC samples studied. The phase compositions of these are summarised in Table 1. Though the samples from both Ranger and Olympic Dam mines were found to be U_3O_8 in the preliminary X-ray analysis (conducted in 2006), the diffraction patterns of sub-samples from the two aged (2017) samples are noticeably different. Analysis of the S-XRD patterns demonstrated that the two samples contained the same three phases, U_3O_8, α-$UO_2(OH)_2$ and α-$(UO_2)_4O(OH)_6{\cdot}5H_2O$ (metaschoepite), however there are significant differences in the relative phase abundances. Interestingly the differences are more significant than evident in the results obtained two years prior using a conventional Cu source (Bruker D8 diffractometer) reported by Ditcham.[10] These differences are highlighted in the supplementary figures S1 to S3. It appears that during prolonged storage the U_3O_8 has reacted with the atmosphere and partially converted to α-$UO_2(OH)_2$ and α-$(UO_2)_4O(OH)_6{\cdot}5H_2O$. The presence of the latter, which is found naturally as the mineral metaschoepite, is consistent with the earlier work of Oerter *et al.*[21] Brugger *et al.* recently described dehydrated schoepite as the mineral species paulscherrerite, with an empirical formula $UO_3{\cdot}1.02(H_2O)$ due to the presence of metaschoepite contaminant. [28, 29]

Tamasi *et al.* [8] reported that ageing synthetic U_3O_8 samples resulted in partial transformation to metaschoepite ($UO_3{\cdot}2H_2O$) and schoepite ($UO_3{\cdot}2.25H_2O$) although they did not quantify the relative amounts of the constitute phases. Interestingly these workers did not report evidence for the formation of α-$UO_2(OH)_2$, which is sometimes described as dehydrated schoepite.[30] Tamasi *et al.* aged their samples for a shorter period, 1-3 years, than the more than 10 years of the present samples. That work, and

the recent study of Hanson *et al*., [17] highlighted that of the three key factors, aging time, temperature and relative humidity identified by Sweet[14] humidity appears to have the greatest impact on the transformations in uranium oxides.

α-$UO_2(OH)_2$ is one of three polymorphs of uranyl di-hydroxide, $UO_2(OH)_2$.[31] The U cation has 8-fold coordination with the hydroxyl groups forming a puckered hexagon that is capped by the uranyl groups. Representative refined structural parameters are given in Table S3.

That the metaschoepite is only a minor phase in the Olympic Dam sample and is considerably more abundant in the Ranger sample is remarkable since the two samples were prepared at around the same time (~ 2005) and have been stored under the same conditions (both in sealed containers in the same laboratory) until the measurements in 2017. It is worth noting that although the Rietveld refinements yield apparently very precise phase compositions, the sample volume analysed in the S-XRD experiments is small leading to the possibility of some variation in phase composition if the sample is not totally homogeneous. Three capillaries were studied for each UOC sample and these results, summarised in Table S5 in the supplementary information, revealed relatively little inhomogeneity. The peaks from the main phases U_3O_8 and α-$UO_2(OH)_2$ were broader than expected from the instrumental resolution. Indeed, it was not possible to directly observe the symmetry lowering from hexagonal to orthorhombic for the U_3O_8 phase. We will return to this point below. Despite the lack of resolved orthorhombic splitting in the profiles the Rietveld refinements returned lattice parameters that are in excellent agreement with values reported previously by Miskowiec *et al.*, Ackermann *et al*., and Loopstra, [26, 32, 33] (Table S1) with the small variation between the Olympic Dam and Ranger samples possibly indicating small differences in the oxygen stoichiometry.

The presence of multiple phases in the UOC sub-samples is presumably a result of the interaction of the surface of the particles with the atmosphere, resulting in a shell of the second phase coating the unreacted core of the initial phase. In such core/shell arrangements the shell phase can be distinguished from the core region by its morphology, chemical composition and/or crystal structure. Broadening of the diffraction peaks for either the core or shell phase

can arise either due to size effects, or it may be a consequence of local strains induced by a mismatch between the core and shell lattice spacings.

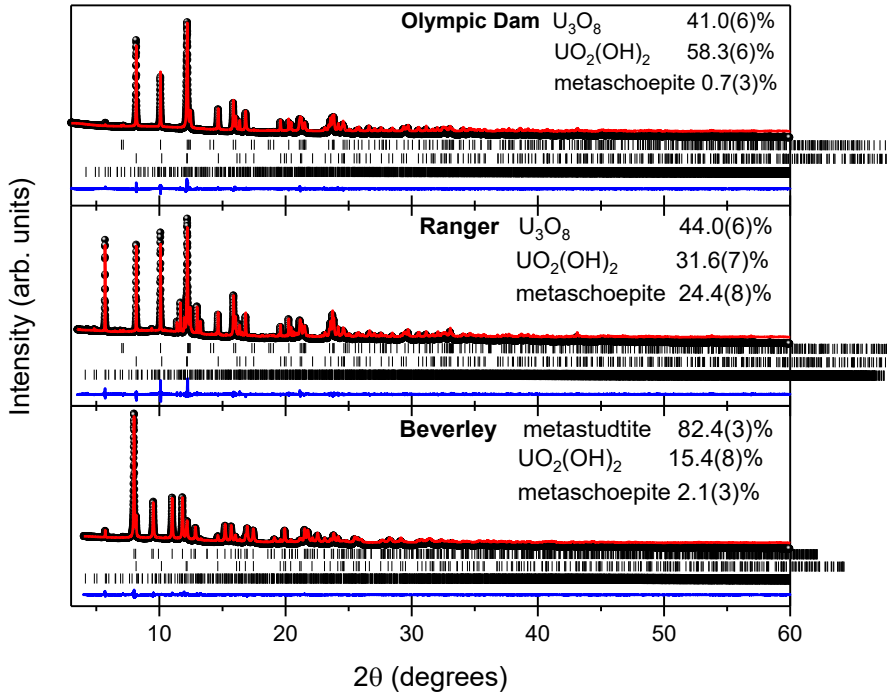

Figure 1. Room temperature S-XRD Rietveld refinement profiles for the three UOC samples studied. In each case the observed data is represented by the symbols, the continuous red line through these is the fit and the lower continuous blue line is the difference between the observed and calculated profiles. The lower tick marks indicate the positions of the space group allowed reflections for the three phases, that are given in the same order as the compositions listed in each panel.

Table 1. Refined structural parameters for the UOC phases obtained by Rietveld analysis against S-XRD data measured at room temperature.

Sample	Phase	Wt %	SG	Lattice Parameters (Å)			Volume (Å^3)
				a	*b*	*c*	
Olympic Dam	U_3O_8	40.98(6)	*C2mm*	6.7200(5)	11.9516(9)	4.1469(3)	333.06(8)
	α-$UO_2(OH)_2$	58.34(6)	*Cmce**	4.2801(3)	10.2346(8)	6.8802(6)	301.39(7)
	metaschoepite	0.68(3)	*Pbcn*	14.628(4)	13.961(4)	16.614(4)	3393.0(14)
Ranger	U_3O_8	44.00(6)	*C2mm*	6.7276(3)	11.9110(6)	4.1438(2)	332.05(5)
	α-$UO_2(OH)_2$	31.63(7)	*Cmce*	4.2793(2)	10.2367(5)	6.8869(3)	301.69(4)
	metaschoepite	24.37(8)	*Pbcn*	14.6779(6)	13.9337(7)	16.6959(8)	3426.9(5)
Beverley	metastudtite	82.44(3)	*Pnma*	8.430(2)	8.787(2)	6.512(1)	482.4(3)
	α-$UO_2(OH)_2$	15.43(8)	*Cmce*	4.2885(8)	10.252(2)	6.901(1)	303.4(2)
	metaschoepite	2.13(3)	*Pbcn*	14.625(3)	13.953(3)	16.559(3)	3379.0(19)

* *Cmce* is the recommended notation for Space Group 64, it replaced *Cmca* which is used in much of the literature.

As anticipated from the preliminary XRD analysis, conducted ~ 10 year prior to the S-XRD measurements, the sample from the Beverley mine contains metastudtite [$UO_2(\eta^2\text{-}O_2)(H_2O)_2$], ($UO_4{\cdot}2H_2O$) together with small amounts of $UO_2(OH)_2$ and metaschoepite. Studtite [$UO_2(\eta^2\text{-}O_2)(H_2O)_2$].$2H_2O$ or $UO_4{\cdot}4H_2O$ and metastudtite [$UO_2(\eta^2\text{-}O_2)(H_2O)_2$] or $UO_4{\cdot}2H_2O$ are the only known naturally occurring uranyl peroxides and have been found on the surface of spent nuclear fuel and on depleted uranium munitions.[34] Thomas *et al.* [35] have reported that studtite transforms to the metastudtite between 75 and 175 ºC and the reactivity of these peroxide species is of potential significance in the design and operation of any geological repository. Mass balance calculations, based on the quantitative phase analysis (QPA) and ideal stoichiometry for the phases, gave the following water contents: Olympic Dam mine 3.6 wt% H_2O, Ranger mine 4.6 wt% H_2O and Beverley mine 10.7 wt% H_2O. These results are in broad agreement with the thermogravimetric analyses of Ditcham *et al*.[10]

The results presented in Table 1 are a powerful illustration of the benefit of high-resolution S-XRD measurements. Ditcham *et al*. in 2016 had suggested the presence of $UO_2(OH)_2$ in the Ranger and Olympic Dam samples but had not quantified the amounts nor had they observed the presence of metaschoepite, despite this phase

representing ~ 5 weight % of the Ranger sample. Likewise, they described Beverley sample as containing studtite $UO_4{\cdot}4H_2O$ and metastudtite $UO_4{\cdot}2H_2O$ and did not comment on the presence of $UO_2(OH)_2$ and metaschoepite.

Structural refinement of metastudtite

We are unaware of any previous high-resolution structural studies of metastudtite. Vitova *et al*. recently reported the structure from refinements against powder diffraction data measured using a conventional (Cu Kα) X-ray source.[36] The cell volume from that work is statistically smaller than that observed here (480.88(7) vs 482.24(18) $Å^3$), see Table S4. The cell volume for metastudtite refined in the present study shows weak thermal expansion on heating from RT to 125 ºC to 482.98(31) $Å^3$, suggesting there is no loss of water over this temperature range. The earlier structural refinements by Vitova *et al*. showed bending of the O=U=O moiety; this is not observed in the present refinements suggesting it was an artefact. [36] The U^{6+} cation in metastudtite is bonded to six oxygen atoms at the equatorial vertices of a distorted bipyramid that is capped by the two oxygens from the linear O=U=O uranyl group, see Figure S8. The O(1)-U-O(2) angle is 178.7(13)º. Four of the equatorial vertices are occupied by O(3) atoms which correspond to two peroxide groups with O-O separation of 1.498(8) Å, the other two sides are occupied by the O(4) atoms of the water molecules. The two uranyl bond distances are not symmetry constrained to be equal and these are found to be statistically different 1.625(16) and 1.864(15) Å. Unequal uranyl bond distances have previously been reported for another uranium peroxide $Na[UO_2(O_2)_3]9H_2O$ as well as in Li_2UO_4.[37 38]

Temperature dependent structures

Having established the phases present in each of the three samples at room temperature the thermal transformations of these were then investigated using *in-situ* S-XRD.

i) Olympic Dam. The weak reflections indexed to the orthorhombic metaschoepite structure (space group *Pbcn*) observed in the sample from the Olympic Dam site were not observed in profiles measured at and above 150 ºC. Finch *et al.* have previously reported that schoepite and metaschoepite can be distinguished by precise determination of unit cell parameters, with the partial loss of water resulting in a contraction of the *b* axis from ~ 14.2 Å to 14.0 Å with very little change in the *a*- and

c-axis.[30] The results presented in Table 1 point to metaschoepite being the appropriate descriptor of the material present in this sample. Metaschoepite loses water when heated above ~ 100 ºC, yielding a material described as "dehydrated schoepite" that appears to have the same structure as α-$UO_2(OH)_2$.[30] Examination of the profiles did not provide any evidence for the appearance of an additional phases around 150 ºC and so we propose that the metaschoepite has transformed to α-$UO_2(OH)_2$.

As the sample was heated to above 300 ºC the peaks from the $UO_2(OH)_2$ phase began to lose intensity, although the absolute intensity of the reflections from the U_3O_8 phase did not change, notwithstanding the coalescence of certain reflections due to the reduction in the orthorhombic splitting. This indicates that the $UO_2(OH)_2$ transformed to an X-ray amorphous phase, rather than to U_3O_8. Although three broad weak unindexed peaks near 2θ =11.95, 21.1 and 21.9 º were observed in the profile measured at 400 ºC it is reasonable to conclude that between 400 and 550 ºC the only crystalline phase present is U_3O_8, and that this is accompanied by an appreciable amount of an amorphous phase.

The profile measured at 550 ºC contains additional reflections that could be indexed to a second orthorhombic phase identified as α-UO_3. As this phase initially forms there is no appreciable change in the intensity of the reflections from the U_3O_8 phase suggesting that the α-UO_3 results from the crystallisation of the amorphous material formed by decomposition of $UO_2(OH)_2$. This hypothesis is supported by the observation that the weight percent of UO_3 in the sample between 600 and 700 ºC is comparable to the amount of $UO_2(OH)_2$ present between 150 and 300 ºC. Around 725 ºC the intensity of the reflections from the α-UO_3 phase begins to diminish and that from the U_3O_8 phase increases showing the conversion of α-UO_3 to U_3O_8 has occurred. Above 800 ºC the profiles were well produced with a single phase hexagonal $P\bar{6}2m$ U_3O_8 model. Cooling the sample from 875 to 100 ºC resulted in the transformation to the orthorhombic $C2mm$ U_3O_8 structure, confirming the $C2mm$ to $P\bar{6}2m$ transition to be reversible as noted by previous workers;[32] no other phases were present in the profile measured at 100 ºC.

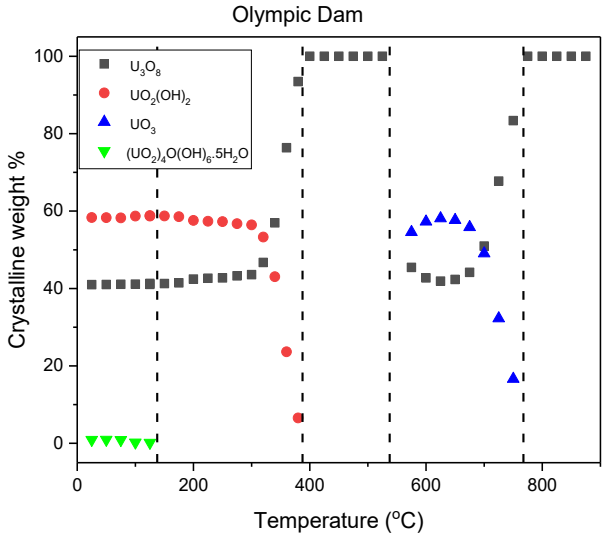

Figure 2. Crystalline weight fraction in Olympic Dam UOC as a function of temperature as estimated by Rietveld refinements. The ESDs from the Rietveld refinements are smaller than the symbols. The contribution of any amorphous material has been neglected in estimating the weight fractions. The dashed vertical lines indicate the temperatures where the phase components of the models used in the Rietveld refinements were altered. Below 400 ºC the U_3O_8 structure is described by the orthorhombic space group *C*2*mm* and above this by the hexagonal space group $P\bar{6}2m$.

The peaks from the main phases U_3O_8 and $UO_2(OH)_2$ were, in the profile measured at room temperature, broader than expected from the instrumental resolution. Indeed, it was not possible to directly observe the symmetry lowering from hexagonal (PG $P\bar{6}2m$) to orthorhombic (SG *C*2*mm*) for the U_3O_8 phase (Figure 3). Such symmetry lowering is clear in the profile measured at 100 ºC after heating the sample to 875 ºC. The broadening of the peaks appears to be a consequence of water adsorption reducing the crystallinity of the material, as evidenced by the observation that a pattern measured in 2006 using a conventional (lower resolution) diffractometer showed diagnostic splitting of the hexagonal (110) reflection near d = 3.415 Å.

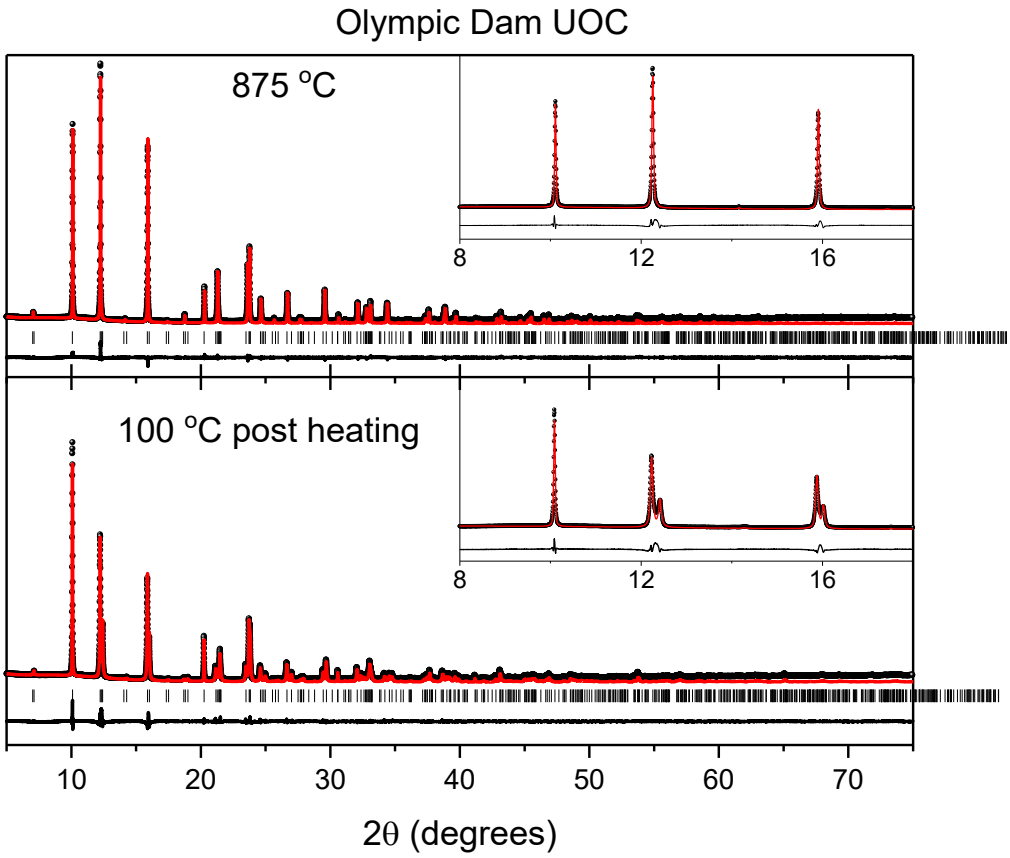

Figure 3. Representative examples of Rietveld refinements for Olympic Dam UOC. Data were collected on heating from RT to 875 ºC and then a small number of patterns were measured on cooling to 100 ºC. The insets highlight the splitting of reflections due to the lowering of symmetry to orthorhombic *C*2*mm* (at 100 ºC) from hexagonal $P\bar{6}2m$ (at 875 ºC).

The thermal expansion of the lattice parameters for the U_3O_8 phase, refined assuming orthorhombic symmetry showed a marked change around 400 ºC, see Figure 4. This is in good agreement with the reported temperature for the orthorhombic to hexagonal phase transition that is reported to occur around 350 ºC.[33] In a separate neutron powder diffraction measurement on a sample of freshly annealed U_3O_8 the transition was observed to occur near 400 ºC. Comparing Figure 4 with Figure 1 of Ackermann *et al*. and Figure 4 of Miskowiec *et al.* confirms the observed anisotropic thermal expansion is a consequence of the phase transition, which is reversible.[32, 33] The orthorhombic *C*2*mm* and hexagonal $P\bar{6}2m$ structures are compared in Figure S12 that highlight these are nearly isomorphic.

The minimum in cell volume of U_3O_8 around 325 ºC was highlighted in the recent study by Miskowiec *et al.*, as was the change around 220 ºC.[33] It was postulated that the latter is associated with an order-disorder transition whereas the former is

associated with the orthorhombic to hexagonal transition. The co-existence of multiple phases in the present sample and the transformations between these, which necessitates changes in the structural model, results in the greater scatter in Figure 5 compared to Figure 4 of Miskowiec *et al.*[33]

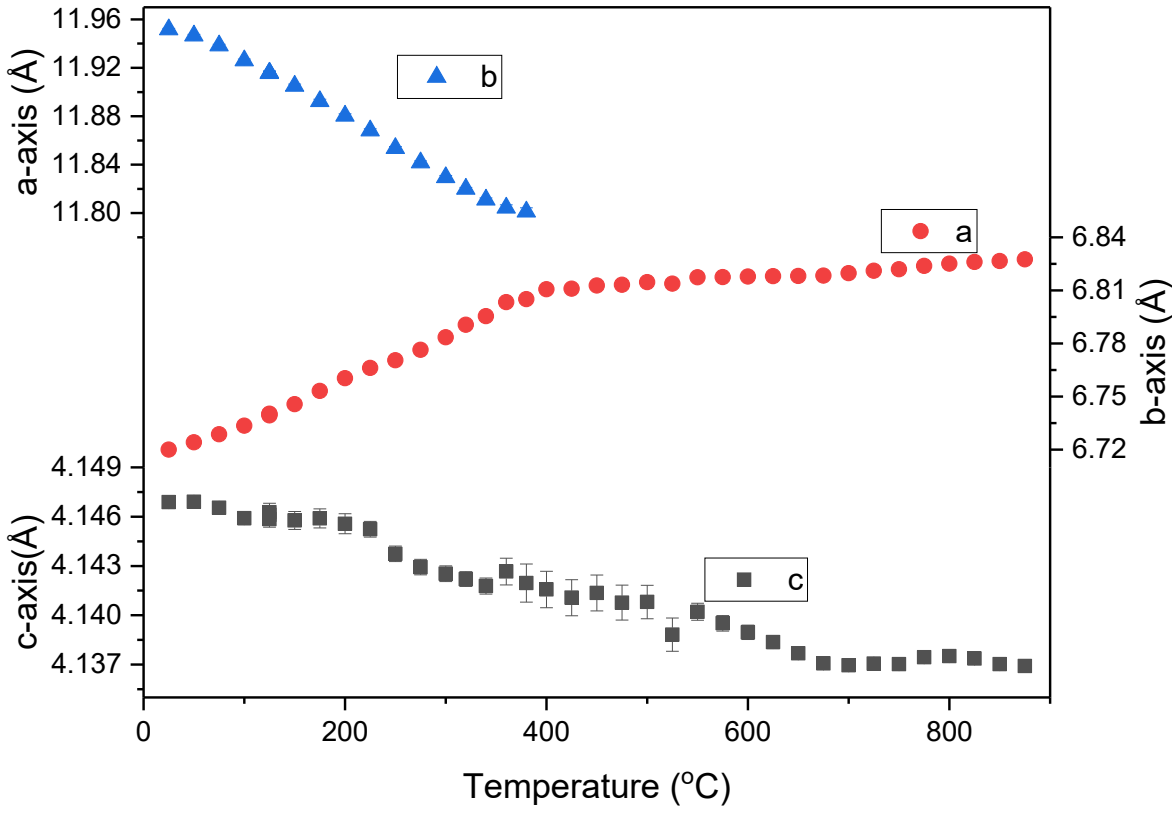

Figure 4. Temperature dependence of the refined lattice parameters for the U_3O_8 phase present in the Olympic Dam UOC sample. The change in the rate of thermal expansion of the a-parameter at 400 ºC is a consequence of the orthorhombic to hexagonal phase transition. The values shown in this figure were from refinements in SG *C*2*mm* below 400 ºC and $P\bar{6}2m$ at 400 ºC and above. Where not apparent the ESDs are smaller than the symbols.

There are no significant changes in the unit cell volume of the U_3O_8 phase between 25 and 875 ºC, see Figure 5. This possibly reflects the very small absolute volume change over this temperature range (~ 0.3%), noting that the minimum in the unit cell volume around 350 ºC mimics that seen in the work on a single phase U_3O_8 sample by Miskowiec and co-workers.[33]

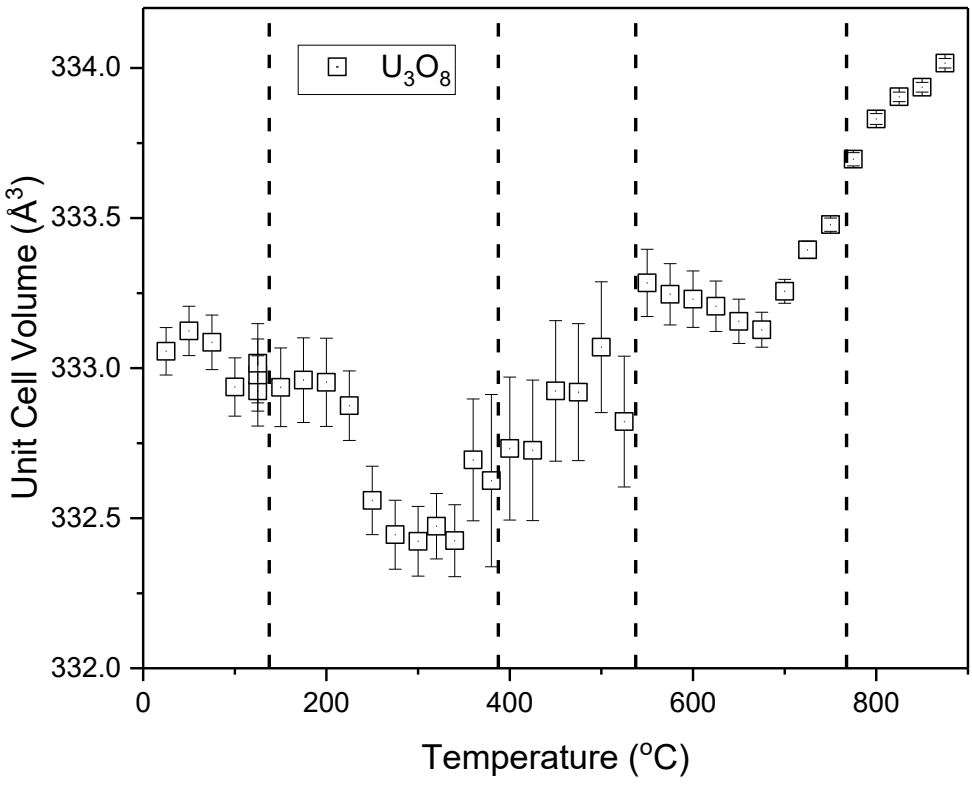

Figure 5. Temperature dependence of the unit cell volume for the U_3O_8 phase present in the Olympic Dam UOC sample. The dashed lines indicate the temperatures where the number or identity of the crystalline phases in the sample changes, requiring a change in the structural model.

ii Ranger. Whilst the absolute crystalline phase weight percentages observed in the Ranger sample are different to that found in the Olympic Dam sample their thermal behaviour is essentially identical. Figure 6 shows the loss of metaschoepite occurs at around 125 ºC as was observed for the Olympic Dam sample. The loss of intensity of the reflections diagnostic of metaschoepite correlates with increased intensity of the reflections due to $UO_2(OH)_2$ validating the earlier assertion that metaschoepite transforms to $UO_2(OH)_2$ at around this temperature. Across this transition the intensity of the reflections diagnostic of U_3O_8 remains essentially unchanged, an observation that is true for all patterns measured from room temperature to around 600 ºC. At approximately 300 ºC the peaks due to $UO_2(OH)_2$ begin to lose intensity and these are no longer observed by 600 ºC. Although this results in an

increase in the crystalline weight percentage of the U_3O_8 phase, the peak intensities from this phase do not significantly change between 300 and 600 ºC indicating that the absolute amount of U_3O_8 remains constant and that the $UO_2(OH)_2$ transforms to an amorphous material. There is an increase in the intensity of the U_3O_8 peaks from around 700 ºC as a consequence of the transformation from UO_3 to U_3O_8.

In summary the diffraction data reveals that metaschoepite transforms to $UO_2(OH)_2$ around 125 ºC. This is presumably associated with the loss of water of crystallisation.[15] At approximately 300 ºC $UO_2(OH)_2$ transforms to an amorphous phase, and this persists to about 600 ºC at which point crystallisation of UO_3 occurs. Finally, above approximately 750 ºC the UO_3 is reduced to U_3O_8. At temperatures above 400 ºC U_3O_8 has a hexagonal structure that distorts to an orthorhombic structure when cooled below this, Figure S4.

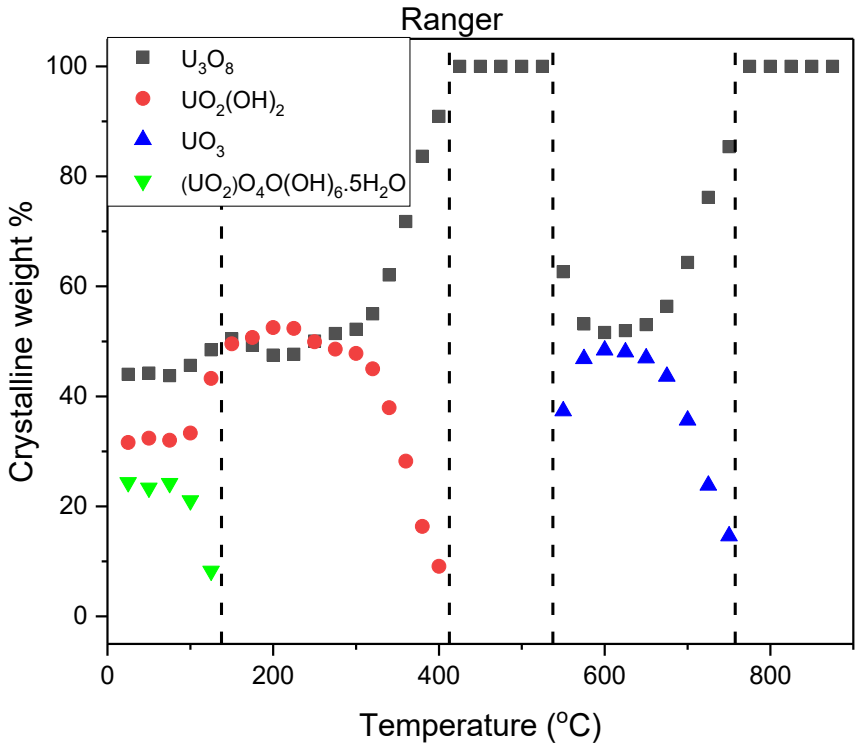

Figure 6. Crystalline weight fraction in Ranger mine UOC as a function of temperature as estimated by Rietveld refinements. The ESDs from the Rietveld refinements are smaller than the symbols. The contribution of any amorphous material has been neglected in estimating the weight fractions. The dashed vertical lines indicate the temperatures where the phase components of the models used in the Rietveld refinements were altered. Below 400 ºC the U_3O_8 structure is described by the orthorhombic space group *C*2*mm* and above this by the hexagonal space group $P\bar{6}2m$.

iii Beverley. As noted above, at room temperature the sample from the Beverley mine consisted of 82.4(3) wt% metastudtite [$UO_2(\eta^2\text{-}O_2)(H_2O)_2$], or $UO_4{\cdot}2H_2O$, 15.4(8) wt% $UO_2(OH)_2$ together with trace amounts, 2.1(3) wt%, of metaschoepite. Heating the sample to around 125 ºC resulted in the loss of the peak near $2\theta = 5.91^{\circ}$ ($d = 7.312$Å), that indexed as the (200) reflection of metaschoepite, which is the strongest peak for this phase.[39] As seen for the Olympic Dam sample there is no change in the intensity of the other peaks at around this temperature, however it is believed that the metaschoepite transforms to α-$UO_2(OH)_2$. Further heating to around 200 ºC results in the loss of intensity of the peaks due to the main metastudtite phase, however this is not accompanied by any significant change in the intensity of the remaining peaks that are from the α-$UO_2(OH)_2$. This indicates that metastudtite transforms to an amorphous material around 200 ºC. It should be stressed that although α-$UO_2(OH)_2$ is the only crystalline phase present between around 250 and 400 ºC, and therefore appears as

100% in Figure 7, based on the observed intensities of the persistent U_3O_8 phase it is believed that only about 15% of the original sample remains crystalline over this temperature range. Continued heating above 400 ºC results in the loss of all resolved peaks and it is not until the sample is heated to above 550 ºC that any well resolved peaks re-emerge. That the α-$UO_2(OH)_2$ phase in the Beverley mine sample becomes amorphous around 400 ºC is consistent with the results described above for the samples from the Ranger and Olympic Dam mines. Odoh *et al.* described heating metastudtite to 200 ºC to form an X-ray amorphous phase they described as U_2O_7.[40] Based on neutron pair distribution function analysis it was concluded that this species retained the peroxide group of the starting phase.[40] Further heating of this U_2O_7 resulted in its decomposition with Odoh *et al.* concluding that UO_3 initially forms before ultimately transforming to U_3O_8. Our observations are consistent with this work, although we cannot comment on the nature of the amorphous species.[41, 42] Attempts to model the profiles measured around 600 ºC to the hexagonal U_3O_8 model were unsuccessful, as there was no evidence for any intensity near 2θ = 7.06º (*d* = 5.917Å) that could be indexed to the hexagonal (100) reflection. It was concluded that this temperature the α-UO_3 structure, that has the orthorhombic *C*2*mm* space group, has formed. Different polymorphs of UO_3 can be obtained by altering the heating conditions,[43] for example flash heating $UO_2(NO_3)\cdot 6H_2O$ in air to 450 °C followed by prolonged annealing at the same temperature is reported to result in the formation of β-UO_3 that has a monoclinic structure. [44]

Independently Tamasi *et al*. described heating $UO_2(O_2).xH_2O$ (studtite) in air to 400 ºC to form amorphous UO_3 (A-UO_3) that transformed to U_3O_8 upon further heating to 800 ºC.[8] It would be interesting to establish if the two amorphous phases contain the same functional groups. Spano and co-workers have recently studied the dehydration of metastudtite and observed the co-existence of mixed-phase UO_x dehydration products of metastudtite and concluded that the decomposition involved the conversion of some uranyl centers from hexagonal to pentagonal bipyramidal coordination units via peroxide liberation.[45] Tamasi *et al*.[46] demonstrated that heating A-UO_3 at 485°C under air for 96 h converted this to α-UO_3; this is a comparable temperature to where the emergence of reflections reappeared in our in-situ diffraction data. As the temperature is progressively increased topotatic reduction of the α-UO_3 phase occurs

resulting in the formation of crystalline U_3O_8 with the hexagonal structure as evident from the appearance of a peak near $2\theta = 7.06^{o}$.

The U_3O_8 phase remains the only crystalline phase present upon cooling the sample back to 100 ºC. It is worth noting that the diffraction pattern measured at 100 ºC for this sample does not show well resolved orthorhombic splitting, Figure 8, suggesting the presence of considerable strain remains in this sample. Although the orthorhombic α-U_3O_8 polymorph is usually observed at room temperature, slow cooling has been shown to result in the formation of β-U_3O_8, the structure of which is described in SG *Cmcm*. β-U_3O_8 has a doubling of the c-axis, and there is no evidence for this in the S-XRD profiles. It is postulated that annealing for a longer period of time would result in the emergence of a highly crystalline sample as was observed for the other two samples studied in this work.

Whereas thermal treatment did not result in any noticeable change in the dark green colour of the two samples obtained from the Olympic Dam and Ranger mines, the Beverley sample showed two distinct colour changes over the heating cycle to 850 °C. The initial yellow sample changed to dark orange on heating to 400 °C, which is consistent with the phase transition to the amorphous phase, and then to dark green as a result of the formation of U_3O_8 phase. These colour changes are evident in the capillaries after analysis (Figure S5).

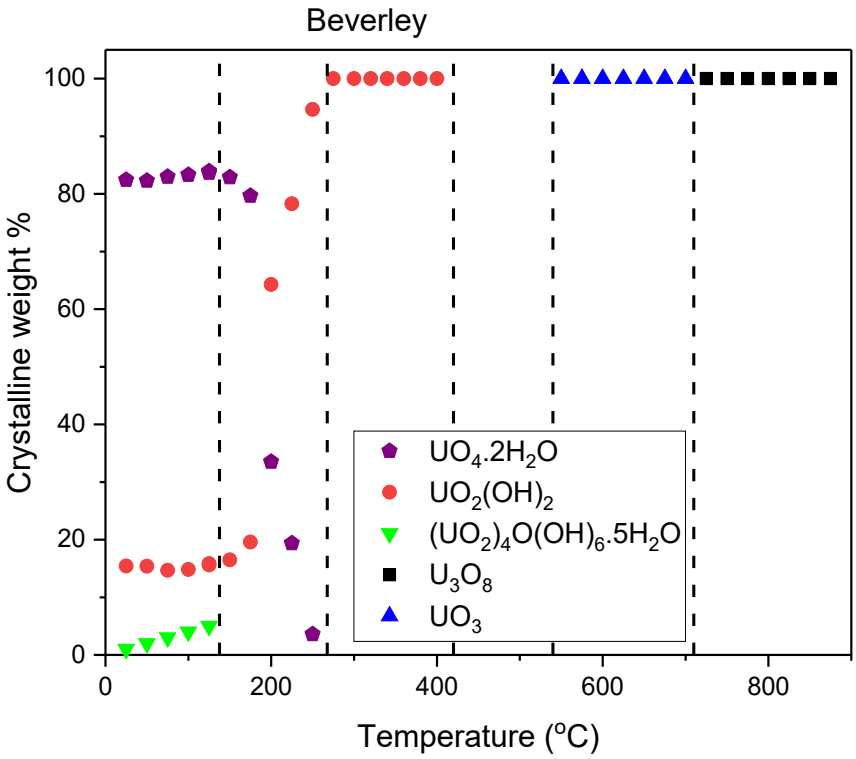

Figure 7. Crystalline weight fraction in Beverley UOC as a function of temperature as estimated by Rietveld refinements. The ESDs from the Rietveld refinements are smaller than the symbols. The contribution of any amorphous material has been neglected in estimating the weight fractions. The dashed vertical lines indicate the temperatures where the phase components of the models used in the Rietveld refinements were altered. Below 400 ºC the U_3O_8 structure is described by the orthorhombic space group *C*2*mm* and above this by the hexagonal space group $P\bar{6}2m$.

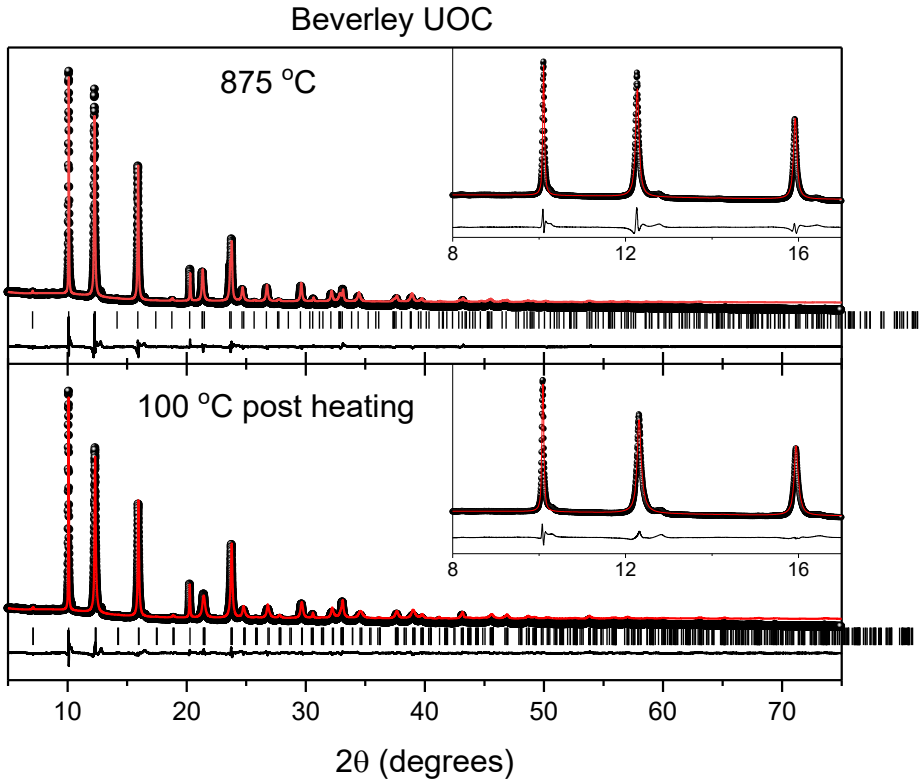

Figure 8. Rietveld refinements for Beverley UOC. Data was collected on heating from RT to 875 ºC and on cooling to 100 ºC. The insets highlight the absence of any noticeable splitting of reflections that are diagnostic of a lowering of symmetry from hexagonal $P\bar{6}2m$ (at 875 ºC) to orthorhombic *C*2*mm* (at 100 ºC).

Table 2. Refined structural parameters for the crystalline phases identified in the three UOC samples. In all cases the listed lattice parameters correspond to the lowest temperature of the quoted range.

Temperature (ºC)	Phase	SG	Lattice Parameters (Å)		
			a	*b*	*c*
Ranger					
25-125	U_3O_8	*C*2*mm*	6.7276(3)	11.9110(6)	4.1438(2)
	$UO_2(OH)_2$	*Cmce*	4.2793(2)	10.2367(5)	6.8869(3)
	metaschoepite	*Pbcn*	14.6779(6)	13.9337(7)	16.6959(8)
150-375	U_3O_8	*C*2*mm*	6.7484(10)	11.8851(16)	4.1449(6)
	$UO_2(OH)_2$	*Cmce*	4.2931(7)	10.2248(15)	6.9235(10)
400-525	U_3O_8	$P\bar{6}2m$	6.8164(16)	6.8164(16)	4.1432(9)
550-750	U_3O_8	$P\bar{6}2m$	6.8181(8)	6.8181(8)	4.1399(5)
	UO_3	*C*2*mm*	3.9593(5)	6.8930(10)	4.1594(5)
750-875	U_3O_8	$P\bar{6}2m$	6.8270(6)	6.8270(6)	4.1383(3)
Olympic Dam					
25-125	U_3O_8	*C*2*mm*	6.7200(5)	11.9516(9)	4.1469(3)
	$UO_2(OH)_2$	*Cmce*	4.2801(3)	10.2346(8)	6.8802(6)

	metaschoepite	*Pbcn*	14.628(4)	13.961(4)	16.614(4)
150-375	U_3O_8	*C*2*mm*	6.7403(9)	11.916(2)	4.1463(5)
	$UO_2(OH)_2$	*Cmce*	4.2970(6)	10.204(1)	6.9239(9)
400-525	U_3O_8	$P\bar{6}2m$	6.8106(19)	6.8106(19)	4.1416(11)
550-750	U_3O_8	$P\bar{6}2m$	6.8174(9)	6.8174(9)	4.1402(5)
	UO_3	*C*2*mm*	3.9717(6)	6.8596(12)	4.1588(5)
750-875	U_3O_8	$P\bar{6}2m$	6.8234(2)	6.8234(2)	4.1378(1)
Beverley					
25-125	metastudtite	*Pnma*	8.430(2)	8.787(2)	6.512(1)
	$UO_2(OH)_2$	*Cmce*	4.2885(8)	10.252(2)	6.901(1)
	metaschoepite	*Pbcn*	14.625(3)	13.953(3)	16.559(3)
150-175	metastudtite	*Pnma*	8.4317(17)	8.7764(18)	6.5259(14)
	$UO_2(OH)_2$	*Cmce*	4.3017(9)	10.220(2)	6.9408(15)
200-360	$UO_2(OH)_2$	*Cmce*	4.2729(6)	10.1570(4)	6.9242(9)
380- 525	Amorphous				
550-700	UO_3	*C*2*mm*	3.9655(12)	6.863(3)	4.11557(13)
725-875	U_3O_8	$P\bar{6}2m$	6.8578(20)	6.8578(20)	4.1664(12)

Conclusions

Rietveld refinement of Synchrotron X-ray diffraction data of UOCs from three Australian uranium mines have undergone alteration and hydration during over a decade of storage under laboratory conditions. The UOC from Olympic Dam and Ranger, which were U_3O_8 when produced have altered to a mixture of U_3O_8, α-$UO_2(OH)_2$ and α-$(UO_2)_4O(OH)_6{\cdot}5H_2O$. The UOC from the Beverley Mine was metastudtite [$UO_2(\eta^2\text{-}O_2)(H_2O)_2$], ($UO_4{\cdot}2H_2O$) when first produced and during prolonged storage has also altered to α-$UO_2(OH)_2$ and α-$(UO_2)_4O(OH)_6{\cdot}5H_2O$. This work has not attempted identify the relative importance of the three key factors influencing the hydrolysis induced transformations in uranium oxides identified by Sweet[14], namely aging time, temperature and relative humidity, and we note that Tamasi *et al.* [8] relative humidity appears to have the greatest impact on the transformations in uranium oxides

The temperature induced phase transitions in the three UOC samples has been established using variable temperature synchrotron X-Ray powder diffraction. Two of the samples, from the Olympic Dam and Ranger mines had been calcined as their final processing step yielding U_3O_8. The third sample from Beverley mine had been precipitated through the addition of peroxide and this produces metastudite [$UO_2(\eta^2\text{-}O_2)(H_2O)_2$], or $UO_4{\cdot}2H_2O$. The thermal behaviour of the aged Olympic Dam and Ranger samples were very similar. At room temperature both samples contained a mixture of three phases namely U_3O_8 (SG *C*2*mm*), α-$UO_2(OH)_2$ (*Cmce*) and metaschoepite $(UO_2)_4O(OH)_6{\cdot}5H_2O$ (*Pbcn*), although the relative abundances of these

three phases were different. The Ranger sample contained much more metaschoepite than the sample sourced from the Olympic Dam mine. Through a combination of Rietveld analysis and examination of the temperature dependence of individual reflections the sequence of transitions in both samples upon heating appears to be metaschoepite decomposes around 125 ºC to an amorphous phase, and α-$UO_2(OH)_2$ also transforms to an amorphous state around 400 ºC. Any similarity between the two amorphous phases formed from metaschoepite or α-$UO_2(OH)_2$ was not established. Around 575 ºC the amorphous material crystallises, initially as α-UO_3 that converts to β-U_3O_8. The co-existence of U_3O_8 and metaschoepite has been noted previously, for example in the work of Tamasi *et al*. Although α-$UO_2(OH)_2$ is described as "dehydrated schoepite" and is reported to be formed by heating metaschoepite to around 450 K (180 ºC) [47] there does not appear to be an obvious topology relationship between the two structures, the metaschoepite structure contains layers of corner-shared pentagonal bipyramids whereas α-$UO_2(OH)_2$ has hexagonal bipyramids.[30]

We propose that metaschoepite develops by the corrosion of the U_3O_8 particles in a core-shell type model. Metaschoepite is described as being stable at room temperature and does not transform to dehydrated schoepite, which is also described as being stable.[30] Thus, it is unlikely that the shell of metaschoepite that forms on the surface of the U_3O_8 crystallites transforms to α-$UO_2(OH)_2$, rather we speculate that it develops at the interface between U_3O_8 and metaschoepite. Irrespective of the mechanism the core-shell model could account for the broadening of the diffraction peaks of the U_3O_8 evident in the samples.

The Beverley UOC sample was predominantly metastudtite ($UO_2{\cdot}2H_2O$ SG *Pnma*) together with small amounts of α-$UO_2(OH)_2$ and metaschoepite. The co-existence of the latter two phases in this sample points to metaschoepite being a precursor to the formation of α-$UO_2(OH)_2$. The *in-situ* diffraction data shows that upon heating the $UO_2{\cdot}2H_2O$ transforms to an amorphous phase, previously described as U_2O_7, and then crystallises as UO_3 before transforming to U_3O_8.

Author Contributions

This manuscript was written through the contributions of all the authors. All authors have given approval to the final version of the manuscript.

The authors declare no competing financial interest.

Acknowledgements

Funding is gratefully acknowledged from Australian Institute of Nuclear Science and Engineering (AINSE) Postgraduate Research Award (Pandelus). This research was undertaken on the Powder Diffraction beamline at the Australian Synchrotron, part of ANSTO (Proposals 12366 and 13376). ANSTO Nuclear Forensics provided the UOC samples. We thank Dr Helen Maynard-Casely for assistance with the neutron diffraction measurements.

Supporting Information

The supporting information contains comparison of S-XRD and convention al XRD profiles, thermal diffractograms for each of the three samples, additional examples of Rietveld refinements, representation of the structures identified in this work tables of refined structural parameters. The material is available free of charge via the internet at htto://pubs.acs.org

References

1. Mayer, K.; Wallenius, M.; Varga, Z., Nuclear Forensic Science: Correlating Measurable Material Parameters to the History of Nuclear Material. *Chemical Reviews* **2013,** *113* (2), 884-900.
2. Pastoor, K. J.; Kemp, R. S.; Jensen, M. P.; Shafer, J. C., Progress in Uranium Chemistry: Driving Advances in Front-End Nuclear Fuel Cycle Forensics. *Inorg. Chem.* **2021,** *https://pubs.acs.org/doi/10.1021/acs.inorgchem.0c03390*.
3. Edwards, C. R.; Oliver, A. J., Uranium processing: A review of current methods and technology. *Jom-Journal of the Minerals Metals & Materials Society* **2000,** *52* (9), 12-20.
4. Varga, Z.; Ozturk, B.; Meppen, M.; Mayer, K.; Wallenius, M.; Apostolidis, C., Characterization and classification of uranium ore concentrates (yellow cakes) using infrared spectrometry. *Radiochimica Acta* **2011,** *99* (12), 807-813.
5. Varga, Z.; Wallenius, M.; Mayer, K.; Keegan, E.; Millett, S., Application of Lead and Strontium Isotope Ratio Measurements for the Origin Assessment of Uranium Ore Concentrates. *Analytical Chemistry* **2009,** *81* (20), 8327-8334.

6. Su, Y.-F.; Tonkyn, R.; Sweet, L.; Corbey, J.; Bryan, S.; Johnson, T., *Characterization of uranium ore concentrate chemical composition via Raman spectroscopy*. SPIE: 2018; Vol. 10629.
7. Wilkerson, M. P.; Hernandez, S. C.; Mullen, W. T.; Nelson, A. T.; Pugmire, A. L.; Scott, B. L.; Sooby, E. S.; Tamasi, A. L.; Wagner, G. L.; Walensky, J. R., Hydration of α-UO_3 following storage under controlled conditions of temperature and relative humidity. *Dalton Transactions* **2020,** *49* (30), 10452-10462.
8. Tamasi, A. L.; Boland, K. S.; Czerwinski, K.; Ellis, J. K.; Kozimor, S. A.; Martin, R. L.; Pugmire, A. L.; Reilly, D.; Scott, B. L.; Sutton, A. D.; Wagner, G. L.; Walensky, J. R.; Wilkerson, M. P., Oxidation and Hydration of U_3O_8 Materials Following Controlled Exposure to Temperature and Humidity. *Analytical Chemistry* **2015,** *87* (8), 4210-4217.
9. Keegan, E.; Richter, S.; Kelly, I.; Wong, H.; Gadd, P.; Kuehn, H.; Alonso-Munoz, A., The provenance of Australian uranium ore concentrates by elemental and isotopic analysis. *Applied Geochemistry* **2008,** *23* (4), 765-777.
10. Ditcham, T. G.; Wotherspoon, A.; Kirkbride, K. P.; Lenehan, C. E.; Popelka-Filcoff, R. S., Thermal decomposition of Australian uranium ore concentrates: characterisation of speciation and morphological changes following thermogravimetric analysis. *Journal of Radioanalytical and Nuclear Chemistry* **2016,** *310* (2), 725-732.
11. Desfougeres, L.; Welcomme, E.; Ollivier, M.; Martin, P. M.; Hennuyer, J.; Hunault, M.; Podor, R.; Clavier, N.; Favergeon, L., Oxidation as an Early Stage in the Multistep Thermal Decomposition of Uranium(IV) Oxalate into U_3O_8. *Inorg. Chem.* **2020,** *59* (12), 8589-8602.
12. Finch, R. J.; Ewing, R. C., The corrosion of uraninite under oxidizing conditions. *Journal of Nuclear Materials* **1992,** *190*, 133-156.
13. Wronkiewicz, D. J.; Bates, J. K.; Wolf, S. F.; Buck, E. C., Ten-year results from unsaturated drip tests with UO_2 at 90 degrees C: Implications for the corrosion of spent nuclear fuel. *Journal of Nuclear Materials* **1996,** *238* (1), 78-95.
14. Sweet, L.; Henager, C.; Hu, S.; Johnson, T.; Meier, D.; Peper, S.; Schwantes, J., *PNNL-20951: Investigation of Uranium Polymorphs*. 2011.
15. Weck, P. F.; Kim, E., Layered uranium(vi) hydroxides: structural and thermodynamic properties of dehydrated schoepite α-$UO_2(OH)_2$. *Dalton Transactions* **2014,** *43* (45), 17191-17199.
16. Wilkerson, M. P.; Hernandez, S. C.; Mullen, W. T.; Nelson, A. T.; Pugmire, A. L.; Scott, B. L.; Sooby, E. S.; Tamasi, A. L.; Wagner, G. L.; Walensky, J. R., Hydration of alpha-UO_3 following storage under controlled conditions of temperature and relative humidity. *Dalton Transactions* **2020,** *49* (30), 10452-10462.
17. Hanson, A. B.; Schwerdt, I. J.; Nizinski, C. A.; Lee, R. N.; Mecham, N. J.; Abbott, E. C.; Heffernan, S.; Olsen, A.; Klosterman, M. R.; Martinson, S.; Brenkmann, A.; McDonald, L. W., Impact of Controlled Storage Conditions on the Hydrolysis and Surface Morphology of Amorphous-UO_3. *ACS Omega* **2021,** *6* (12), 8605-8615.
18. Hanson, A. B.; Lee, R. N.; Vachet, C.; Schwerdt, I. J.; Tasdizen, T.; McDonald, L. W., Quantifying Impurity Effects on the Surface Morphology of α-U_3O_8. *Analytical Chemistry* **2019,** *91* (15), 10081-10087.

19. Nizinski, C. A.; Hanson, A. B.; Fullmer, B. C.; Mecham, N. J.; Tasdizen, T.; McDonald, L. W., Effects of process history on the surface morphology of uranium ore concentrates extracted from ore. *Minerals Engineering* **2020,** *156*, 106457.
20. Brugger, J.; Meisser, N.; Etschmann, B.; Ansermet, S.; Pring, A., Paulscherrerite from the Number 2 Workings, Mount Painter Inlier, Northern Flinders Ranges, South Australia: "Dehydrated schoepite" is a mineral after all. *Am. Miner.* **2011,** *96* (2-3), 229-240.
21. Oerter, E. J.; Singleton, M.; Dai, Z. R.; Deinhart, A.; Thaw, M.; Davisson, M. L., Hydrogen and oxygen stable isotope composition of water in metaschoepite mineralization on U_3O_8. *Applied Geochemistry* **2020,** *112*.
22. Wallwork, K. S.; Kennedy, B. J.; Wang, D., The high resolution powder diffraction beamline for the Australian Synchrotron. In *Synchrotron Radiation Instrumentation, Pts 1 and 2*, Choi, J. Y.; Rah, S., Eds. Amer Inst Physics: Melville, 2007; Vol. 879, pp 879-882.
23. Larson, A. C.; Von Dreele, R. B. *General Structure Analysis System (GSAS)*; Los Alamos National Laboratory, 1994.
24. Toby, B. H., EXPGUI, a graphical user interface for GSAS. *Journal of Applied Crystallography* **2001,** *34*, 210-213.
25. Weller, M. T.; Light, M. E.; Gelbrich, T., Structure of uranium(VI) oxide dihydrate, $UO_3.2H_2O$; synthetic meta-schoepite $(UO_2)_4O(OH)_6.5H_2O$. *Acta Crystallographica Section B* **2000,** *56* (4), 577-583.
26. Loopstra, B. O., Neutron diffraction investigation of U_3O_8. *Acta Crystallographica* **1964,** *17* (6), 651-654.
27. Weck, P. F.; Kim, E.; Jove-Colon, C. F.; Sassani, D. C., Structures of uranyl peroxide hydrates: a first-principles study of studtite and metastudtite. *Dalton Transactions* **2012,** *41* (32), 9748-9752.
28. Brugger, J.; Meisser, N.; Etschmann, B.; Ansermet, S.; Pring, A., Paulscherrerite from the Number 2 Workings, Mount Painter Inlier, Northern Flinders Ranges, South Australia: “Dehydrated schoepite” is a mineral after all *American Mineralogist* **2011,** *96* (2-3), 229-240.
29. Wronkiewicz, D. J.; Buck, E. C., Uranium Mineralogy and the Geologic Disposal of Spent Nuclear Fuel. *Reviews in Mineralogy <D>* **1999,** *38*, 475-497.
30. Finch, R. J.; Hawthorne, F. C.; Ewing, R. C., Structural relations among schoepite, metaschoepite and "dehydrated schoepite". *Can. Mineral.* **1998,** *36*, 831-845.
31. Siegel, S.; Hoekstra, H. R.; Gebert, E., The structure of γ-uranyl dihydroxide, $UO_2(OH)_2$. *Acta Crystallographica Section B* **1972,** *28* (12), 3469-3473.
32. Ackermann, R. J.; Chang, A. T.; Sorrell, C. A., Thermal expansion and phase transformations of the U_3O_{8-z} phase in air. *Journal of Inorganic and Nuclear Chemistry* **1977,** *39* (1), 75-85.
33. Miskowiec, A.; Spano, T.; Hunt, R.; Shields, A. E.; Niedziela, J. L.; Finkeldei, S., Structural features of solid-solid phase transitions and lattice dynamics in U_3O_8. *Physical Review Materials* **2020,** *4* (9), 093610.
34. Wang, Y.; von Gunten, K.; Bartova, B.; Meisser, N.; Astner, M.; Burger, M.; Bernier-Latmani, R., Products of in Situ Corrosion of Depleted Uranium Ammunition in Bosnia and Herzegovina Soils. *Environmental Science & Technology* **2016,** *50* (22), 12266-12274.
35. Thomas, R.; Rivenet, M.; Berrier, E.; de Waele, I.; Arab, M.; Amaraggi, D.; Morel, B.; Abraham, F., Thermal decomposition of $(UO_2)O_2(H_2O)_2{\cdot}2H_2O$: Influence

on structure, microstructure and hydrofluorination. *Journal of Nuclear Materials* **2017,** *483*, 149-157.
36. Vitova, T.; Pidchenko, I.; Biswas, S.; Beridze, G.; Dunne, P. W.; Schild, D.; Wang, Z.; Kowalski, P. M.; Baker, R. J., Dehydration of the Uranyl Peroxide Studtite, $[UO_2(\eta^2\text{-}O_2)(H_2O)_2]\cdot 2H_2O$, Affords a Drastic Change in the Electronic Structure: A Combined X-ray Spectroscopic and Theoretical Analysis. *Inorg. Chem.* **2018,** *57* (4), 1735-1743.
37. Alcock, N. W., The crystal and molecular structure of sodium uranyl triperoxide. *Journal of the Chemical Society A: Inorganic, Physical, Theoretical* **1968,** (0), 1588-1594.
38. Gebert, E.; Hoekstra, H. R.; Reis, A. H.; Peterson, S. W., The crystal structure of lithium uranate. *Journal of Inorganic and Nuclear Chemistry* **1978,** *40* (1), 65-68.
39. Hawthorne, F.; Finch, R.; Ewing, R., Schoepite and Dehydrated Schoepite. *MRS Proceedings* **2011,** *412*.
40. Odoh, S. O.; Shamblin, J.; Colla, C. A.; Hickam, S.; Lobeck, H. L.; Lopez, R. A. K.; Olds, T.; Szymanowski, J. E. S.; Sigmon, G. E.; Neuefeind, J.; Casey, W. H.; Lang, M.; Gagliardi, L.; Burns, P. C., Structure and Reactivity of X-ray Amorphous Uranyl Peroxide, U2O7. *Inorg. Chem.* **2016,** *55* (7), 3541-3546.
41. Brincat, N. A.; Parker, S. C.; Molinari, M.; Allen, G. C.; Storr, M. T., Ab Initio Investigation of the UO_3 Polymorphs: Structural Properties and Thermodynamic Stability. *Inorg. Chem.* **2014,** *53* (23), 12253-12264.
42. Leinders, G.; Bes, R.; Kvashnina, K. O.; Verwerft, M., Local Structure in U(IV) and U(V) Environments: The Case of U_3O_7. *Inorg. Chem.* **2020,** *59* (7), 4576-4587.
43. Manaud, J.; Maynadie, J.; Mesbah, A.; Hunault, M.; Martin, P. M.; Zunino, M.; Meyer, D.; Dacheux, N.; Clavier, N., Hydrothermal Conversion of Uranium(IV) Oxalate into Oxides: A Comprehensive Study. *Inorg. Chem.* **2020,** *59* (5), 3260-3273.
44. Spano, T. L.; Shields, A. E.; Barth, B. S.; Gruidl, J. D.; Niedziela, J. L.; Kapsimalis, R. J.; Miskowiec, A., Computationally Guided Investigation of the Optical Spectra of Pure beta-UO_3. *Inorg. Chem.* **2020,** *59* (16), 11481-11492.
45. Spano, T. L.; Niedziela, J. L.; Shields, A. E.; McFarlane, J.; Zirakparvar, A.; Brubaker, Z.; Kapsimalis, R. J.; Miskowiec, A., Structural, Spectroscopic, and Kinetic Insight into the Heating Rate Dependence of Studtite and Metastudtite Dehydration. *The Journal of Physical Chemistry C* **2020,** *124* (49), 26699-26713.
46. Tamasi, A. L.; Cash, L. J.; Mullen, W. T.; Pugmire, A. L.; Ross, A. R.; Ruggiero, C. E.; Scott, B. L.; Wagner, G. L.; Walensky, J. R.; Wilkerson, M. P., Morphology of U_3O_8 materials following storage under controlled conditions of temperature and relative humidity. *Journal of Radioanalytical and Nuclear Chemistry* **2017,** *311* (1), 35-42.
47. Hoekstra, H. R.; Siegel, S., Uranium trioxide-water system. *Journal of Inorganic & Nuclear Chemistry* **1973,** *35* (3), 761-779.

For Table of Contents Only

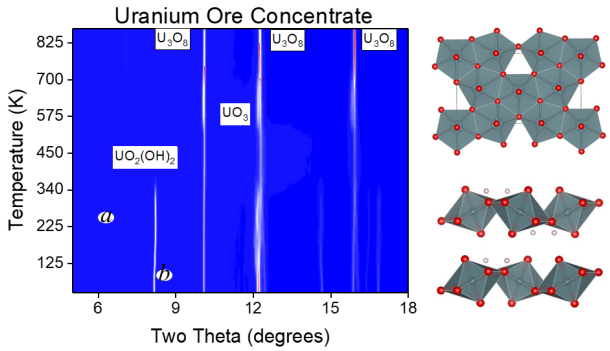

The major phases present within three aged uranium ore concentrates and the temperature induced phase transitions of these were determined using high energy synchrotron X-ray diffraction.